Dept. of Mech. Eng.
CUET

Published Online March 2015 (http://www.cuet.ac.bd/merj/index.html)

Mechanical Engineering Research Journal

Vol. 9, pp. 7–12, 2013

ISSN: 1990-5491

BUOYANT FLOW OF NANOFLUID FOR HEAT-MASS TRANSFER THROUGH A THIN LAYER

R. Nasrin*, S. Parvin and M. A. Alim

Department of Mathematics, Bangladesh University of Engineering and Technology, Dhaka - 1000, Bangladesh

Abstract: To represent the mass, momentum, energy and concentration conservations of the nanofluid medium inside a thin wavy layer the pressure-velocity form of Navier-Stokes equations, energy equation and concentration equation are used. The governing equations and corresponding boundary conditions are converted to dimensionless form and solved numerically by finite element method with discretization by triangular mesh elements with six nodes. The wavy layer is assumed to be filled with water based nanofluid with copper (Cu) nanoparticles. The study includes computations for different values of buoyancy ratio (*Nr* = 1, 5, 10 and 15). Flow, heat and mass transfer characteristics are presented in terms of streamlines, isotherms and iso-concentrations. In addition, results for the average heat and mass transfer, mean temperature and concentration of nanofluid and sub domain average velocity field are offered and discussed for the above mentioned parametric condition. Results show that the effect of *Nr* on the convective heat and mass transfer phenomenon inside the layer are significant. Greater heat and mass transfer rates are observed for the highest value of *Nr*. The numerical validation shows excellent concurrence with the hypothetical outcome.

Keywords: *Buoyant flow, heat-mass transfer, thin wavy layer, finite element method, water/Cu nanofluid.*

NOMENCLATURE

Symbol	Meaning	Unit
c	Concentration	(kg/m^3)
C	Concentration	Dimentionless
C_p	Specific heat at constant pressure	(J/kgK)
C_s	Concentration susceptibility	(m^3/kg)
D	Solutal diffusivity	(m^2/s)
Df	Dufour parameter	Dimentionless
g	Gravitational acceleration	(m/s^2)
h	Local heat transfer coefficient	(W/m^{2}K)
k	Thermal conductivity	(W/mK)
L	Length of the thin layer	(m)
Nr	Buoyancy ratio	Dimentionless
Nu	Nusselt number	Dimentionless
Pr	Prandtl number	Dimentionless
Ra_c	Solutal Rayleigh number	Dimentionless
Ra_T	Thermal Rayleigh number	Dimentionless
Sc	Schmidt number	Dimentionless
Sh	Sherwood number	Dimentionless
Sr	Soret parameter	Dimentionless
T	temperature	(K)
T_i	Initial temperature of nanofluid	(K)
u, v	x and y components of velocity	(m/s)
U, V	x and y components of velocity	Dimentionless
x, y	coordinates	(m)
X, Y	coordinates	Dimentionless
Greek Symbols		
α	Fluid thermal diffusivity	(m^2/s)
β_T	Thermal expansion coefficient	(1/K)
β_C	Solutal expansion coefficient	(1/K)
ϕ	Nanoparticles volume fraction	Dimentionless
ν	Kinematic viscosity	(m^2/s)
θ	temperature	Dimentionless
ρ	Density	(kg/m^3)
μ	Dynamic viscosity	(Ns/m^2)
Subscripts		
av	mean	
c	cold	
f	fluid	
h	hot	
s	solid particle	

* **Corresponding author:** Email: rehena@math.buet.ac.bd; Tel: +88-01766924295; Fax: +88-02-8613046

1. INTRODUCTION

The fluids with solid-sized nanoparticles suspended in them are called “nanofluids”. Applications of nanoparticles in thermal field are to augment warmth transport from solar collectors to luggage compartment tanks, to pick up proficiency of coolants in transformers.

The natural convection in enclosures continues to be a very active area of research during the past few decades. Solar collectors are key elements in many applications, such as building heating systems, solar drying devices etc.

Double diffusive natural convection in a partially heated enclosure using nanofluid was studied by Parvin et al. [1] where the effect of the parameters namely Rayleigh number and solid volume fraction of nanoparticle on the flow pattern and heat and mass transfer had been depicted. Parvin et al. [2] analyzed heat transfer through direct absorption solar collector. Nasrin et al. [3–12] studied various effects of natural convective heat and mass transfers of nanofluid inside two types of solar collectors. They also investigated performance of different nanofluids in heat transfer with different geometries. Here the authors solved the governing partial differential equations with proper boundary conditions by the Finite Element Method using Galerkin’s weighted residual scheme.

From the literature review it is mentioned that a few numerical or experimental works have been done introducing nanofluid for the purpose of heat and mass transfer. The convective phenomenon for the effect of buoyancy ratio is studied through the wavy layer utilizing water based nanofluid with Cu nanoparticle from the current study. So, the authors want to present flow, temperature and concentration augmentation by nanofluid inside a wavy thin layer.

2. GEOMETRICAL MODELING

The graphical representation of a corrugated nanofluid layer is expressed in the Fig. 1. The liquid inside the layer is water-based nanofluid including Cu nanoparticle. The nanofluid is considered incompressible and the flow is assumed as laminar. It is taken that base fluid and nanoparticle are in thermal balance and no slip maintains among them. In this investigation, the top and bottom surfaces are maintained at constant temperatures T_h and T_c respectively where $T_h > T_c$. The vertical walls are perfectly insulated. The concentration in top wall is maintained higher than bottom wall ($C_c < C_h$). The concentration of the nanofluid is observed by the Boussinesq form. It is assumed that the nanoparticle is spherical in shape and diameters are 5 nm. An amplitude of wave A_m = 0.04 and number of wave λ = 3.5 are assumed for the bottom corrugated surface.

3. MATHEMATICAL MODELING

The leading equations for laminar buoyancy convective flow inside a thin corrugated layer utilized by water-based nanofluid with Cu nanoparticle in terms of the Navier-Stokes and energy equation (dimensional form) are given as

Continuity equation:

$$\frac{\partial u}{\partial x}+\frac{\partial v}{\partial y}=0 \tag{1}$$

Momentum conservation equations:

$$\rho_{nf}\left(u\frac{\partial u}{\partial x}+v\frac{\partial u}{\partial y}\right)=-\frac{\partial p}{\partial x}+\mu_{nf}\left(\frac{\partial^2 u}{\partial x^2}+\frac{\partial^2 u}{\partial y^2}\right) \tag{2}$$

$$\begin{aligned}\rho_{nf}\left(u\frac{\partial v}{\partial x}+v\frac{\partial v}{\partial y}\right)=&-\frac{\partial p}{\partial y}+\mu_{nf}\left(\frac{\partial^2 v}{\partial x^2}+\frac{\partial^2 v}{\partial y^2}\right)\\&+g\rho_{nf}\beta_{nf}\left\{(T-T_c)+(c-C_c)\right\}\end{aligned} \tag{3}$$

Energy conservation equation:

$$u\frac{\partial T}{\partial x}+v\frac{\partial T}{\partial y}=\alpha_{nf}\left(\frac{\partial^2 T}{\partial x^2}+\frac{\partial^2 T}{\partial y^2}\right)+\frac{D_f K_{Tf}}{C_s C_p}\left(\frac{\partial^2 c}{\partial x^2}+\frac{\partial^2 c}{\partial y^2}\right) \tag{4}$$

Concentration conservation equation:

$$u\frac{\partial c}{\partial x}+v\frac{\partial c}{\partial y}=D_{nf}\left(\frac{\partial^2 c}{\partial x^2}+\frac{\partial^2 c}{\partial y^2}\right)+\frac{D_f K_{Tf}}{T_m}\left(\frac{\partial^2 T}{\partial x^2}+\frac{\partial^2 T}{\partial y^2}\right) \tag{5}$$

where, $\rho_{nf}=(1-\phi)\rho_f+\phi\rho_s$ is the density,

$(\rho cp)_{nf}=(1-\phi)(\rho cp)_f+\phi(\rho cp)_s$ is the heat capacitance,

$(\rho\beta)_{nf}=(1-\phi)(\rho\beta)_f+\phi(\rho\beta)_s$ is the thermal expansion coefficient and

$\alpha_{nf}=k_{nf}/(\rho cp)_{nf}$ is the thermal diffusivity.

In the current study, the viscosity of the nanofluid is considered by the Pak and Cho correlation [13]. This correlation is given as

$$\mu_{nf}=\mu_f\left\{1+39.11\phi+533.9\phi^2\right\} \tag{6}$$

The effective thermal conductivity of the nanofluid is approximated by the Maxwell-Garnett model [11]:4

$$k_{nf}=k_f\frac{k_s+2k_f-2\phi(k_f-k_s)}{k_s+2k_f+\phi(k_f-k_s)} \tag{7}$$

The boundary conditions are: at all solid borders: $u = v = 0$ at the top surface: $T = T_h$, $c = C_h$; at the vertical walls: $\frac{\partial T}{\partial x}=0,\ \frac{\partial c}{\partial x}=0$; at the bottom wavy wall: $T = T_c$, $c = C_c$

The previous equations become dimensionless by means of the subsequent non-dimensional reliant and free variables:

$$X=\frac{x}{L},\quad Y=\frac{y}{L},\quad U=\frac{uL}{\nu_f},\quad V=\frac{vL}{\nu_f},$$

$$P=\frac{pL^2}{\rho_f{\nu_f}^2},\quad \theta=\frac{T-T_c}{T_w-T_c},\ C=\frac{c-C_c}{C_h-C_c}$$

Then the dimensionless governing equations are

$$\frac{\partial U}{\partial X}+\frac{\partial V}{\partial Y}=0 \tag{8}$$

$$U\frac{\partial U}{\partial X}+V\frac{\partial U}{\partial Y}=-\frac{\rho_f}{\rho_{nf}}\frac{\partial P}{\partial X}+\frac{\nu_{nf}}{\nu_f}\left(\frac{\partial^2 U}{\partial X^2}+\frac{\partial^2 U}{\partial Y^2}\right) \quad (9)$$

$$U\frac{\partial V}{\partial X}+V\frac{\partial V}{\partial Y}=-\frac{\rho_f}{\rho_{nf}}\frac{\partial P}{\partial Y}+\frac{\nu_{nf}}{\nu_f}\left(\frac{\partial^2 V}{\partial X^2}+\frac{\partial^2 V}{\partial Y^2}\right)+\frac{Ra_c}{Pr}\frac{(1-\phi)(\rho\beta)_f+\phi(\rho\beta)_s}{\rho_{nf}\beta_f}(Nr\,\theta+C) \quad (10)$$

$$U\frac{\partial \theta}{\partial X}+V\frac{\partial \theta}{\partial Y}=\frac{1}{Pr}\frac{\alpha_{nf}}{\alpha_f}\left(\frac{\partial^2 \theta}{\partial X^2}+\frac{\partial^2 \theta}{\partial Y^2}\right)+Df\left(\frac{\partial^2 C}{\partial X^2}+\frac{\partial^2 C}{\partial Y^2}\right) \quad (11)$$

$$U\frac{\partial C}{\partial X}+V\frac{\partial C}{\partial Y}=\frac{1}{Sc}\frac{D_{nf}}{D_f}\left(\frac{\partial^2 C}{\partial X^2}+\frac{\partial^2 C}{\partial Y^2}\right)+Sr\left(\frac{\partial^2 \theta}{\partial X^2}+\frac{\partial^2 \theta}{\partial Y^2}\right) \quad (12)$$

where $Pr=\left(\frac{\nu}{\alpha}\right)_f$ is the Prandtl number,

$Ra_T=\frac{g\beta_{Tf}L^3(T_w-T_c)}{\nu_f\alpha_f}$ is the thermal Rayleigh number,

$Ra_c=\frac{g\beta_{cf}L^3(C_h-C_c)}{\nu_f\alpha_f}$ is the solutal Rayleigh number,

$Nr=\frac{Ra_T}{Ra_c}$ is the buoyancy ratio number,

$Df=\left(\frac{D}{\nu}\right)_f\frac{k_{Tf}(C_h-C_c)}{C_sC_p(T_w-T_c)}$ is the Dufour coefficient,

$Sr=\left(\frac{D}{\nu}\right)_f\frac{k_{Tf}(T_w-T_c)}{T_m(C_h-C_c)}$ is the Soret coefficient and

$Sc=\left(\frac{\nu}{D}\right)_f$ is the Schmidt number.

The consequent border situations get the form: at all solid borders: $U = V = 0$; at the wavy surface: $\theta = 0$, $C = 0$; at the top wall: $T = 1$, $C = 1$; at the vertical surfaces: $\frac{\partial\theta}{\partial X}=0, \frac{\partial C}{\partial X}=0$

The local convective Nusselt number of the fluid at the top heated surface is

$$\overline{Nu_c}=-\frac{k_{nf}}{k_f}\frac{\partial\theta}{\partial Y}.$$

With the integration of the local Nusselt number over the inclined heated surface, the mean convective heat transfer at the heated wall of the thin layer is used by Saleh et al. [15] as

$$Nu=\int_0^1\overline{Nu}\,dX.$$

The average Sherwood number at the concentrated surface of the nanofluid layer is defined as

$$Sh=-\int_0^1\frac{k_{nf}}{k_f}\frac{\partial C}{\partial X}dX$$

The mean bulk temperature, concentration and average sub domain velocity of the fluid inside the nanofluid layer may be written as

$\theta_{av}=\int\theta\,d\bar{V}/\bar{V}$, $C_{av}=\int C\,d\bar{V}/\bar{V}$ and $V_{av}=\int V\,d\bar{V}/\bar{V}$, where V and $\bar{V}$ are the magnitude of dimensionless velocity vector and volume of the undulating layer.

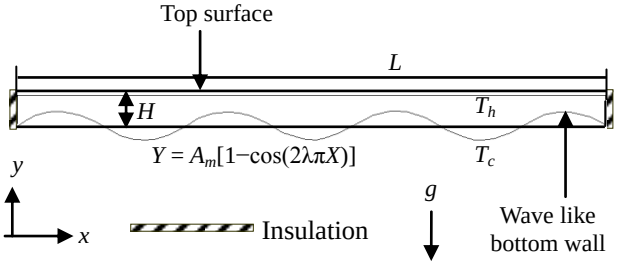

Fig.1: Schematic diagram of the thin layer.

3. NUMERICAL IMPLEMENTATION

The Galerkin finite element method [16,17] is used to solve the non-dimensional governing equations along with boundary conditions for the considered problem. The equation of continuity has been used as a constraint due to mass conservation and this restriction may be used to find the pressure distribution. The finite element method is used to solve the Eqs. (9) - (12), where the pressure P is eliminated by a constraint. The continuity equation (8) is automatically fulfilled for large values of this penalty constraint. Then the velocity components (U, V), temperature (θ) and concentration (C) are expanded using a basis set. The Galerkin finite element technique yields the subsequent nonlinear residu al equations. Three points Gaussian quadrature is used to evaluate the integrals in these equations. The non-linear residual equations are solved using Newton–Raphson method to determine the coefficients of the expansions. The convergence of solutions is assumed when the relative error for each variable between consecutive iterations is recorded below the convergence criterion ε such that $\left|\psi^{n+1}-\psi^n\right|\le 10^{-4}$, where n is the number of iteration and Ψ is a function of U, V, θ and C.

4.1. Thermo-physical properties

The thermo-physical properties of the nanofluid are taken from Ogut [18] and given in Table 1.

Table 1 Thermo-physical properties of water-Cu nanofluid

Physical Properties	Fluid phase (water)	Cu
C_p(J/kgK)	4179	385
ρ (kg/m^3)	997.1	8933
k (W/mK)	0.613	400
$\alpha\times10^7$ (m^2/s)	1.47	1163.1
$\beta\times10^5$ (1/K)	21	5.1

4.2. Grid Independent Test

For Pr = 6.2, Df = 0.5, Sr = 0.3, Sc = 1, Nr = 1, $Ra_T = 10^4$, ϕ = 5% in a solar collector, a widespread mesh solution process is performed to assurance grid-independent test. We inspect five special non-uniform grid schemes with the subsequent number

of elements inside the declaration sector: 2969, 5130, 6916, 9057, and 11426 in the present work. For the above mentioned elements to build up an accepting of the grid excellence the mathematical system is brought for extremely accurate type in the mean Nusselt numbers namely *Nu*, and *Sh* average Sherwood number *Sh*. It is exposed in Table 2. The level of the mean Nusselt number and Sherwood number for 9057 elements exposes a small variation with the outcome attained for the other elements. Hence, allowing for the non-uniform grid scheme of 9057 elements is chosen for the calculation.

Table 2 Grid Test at Pr = 6.2, Df = 0.5, Sr = 0.3, Sc = 1, Nr = 1, $Ra_T = 10^4$, ϕ = 5%

Nodes (elements)	6224 (2969)	10982 (5130)	13538 (6916)	20295 (9057)	27524 (11426)
Nu	6.83	7.98	8.77	9.27	9.28
Sh	5.59	6.76	7.68	8.48	8.50
Time (s)	226.26	292.60	388.16	421.33	627.37

4.3. Code Validation

The present code results for average Nusselt (*Nu*) and Sherwood (*Sh*) numbers with the variation of thermal Rayleigh number (Ra_T) using $D_f = S_r$ = 0.5, Sc = 5 and Pr = 11.573 with the graphical demonstration of Nithyadevi and Yang [19]. The comparison is demonstrated in the Fig. 2.

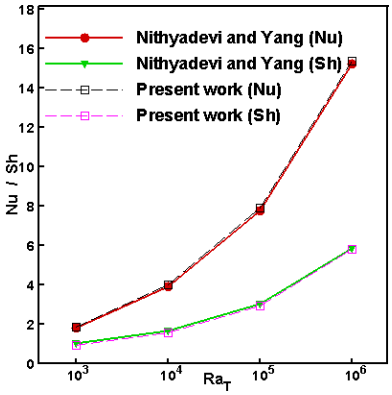

Fig. 2: Comparison between present code and Nithyadevi and Yang using [19] R = 0.5, N = 1, $D_f = S_r$ = 0.5 and Sc = 5.

5. RESULTS AND DISCUSSION

For different buoyancy ratio (*Nr*) numerical investigations of velocity, temperature and concentration with water based nanofluid having copper nanoparticle through a wavy thin layer are displayed. The solid volume fractions ϕ = 5%, Prandtl number Pr = 6.2, Dufour coefficient Df = 0.5, Soret coefficient Sr = 0.3, thermal Rayleigh number $Ra_T = 10^4$ and Schmidth number Sc = 1 are kept fixed. The considered values of buoyancy ratio are *Nr* (= 1, 5, 10 and 15). Also, for the above mentioned parameter, the mean Nusselt number, mean Sherwood number as well as mean bulk temperature, concentration and average sub domain velocity profile inside the layer are revealed graphically. In the streamlines (figure 3(c)) the right and left vortices in each wave rotate in anticlockwise and clockwise directions respectively.

The effect of *Nr* on the thermal, concentration and flow fields is presented in Figs. 3(a)-(c). In the isotherms, iso-concentrations and streamlines (Figs. 3(a)-(c)) the red colored solid lines indicate water based nanofluid and the black colored dashed lines indicate the base fluid. In fluid mechanics, the Rayleigh number (*Ra*) itself may also be viewed as the ratio of buoyancy and viscosity forces times the ratio of momentum and thermal diffusivities. The thermal Rayleigh number (Ra_T) for a fluid is a dimensionless number associated with buoyancy driven flow. Heat transfer is primarily in the form of convection due to temperature gradient. The solutal Rayleigh number (Ra_C) is also dimensionless number and the mass transfer is in the form of convection due to density gradient. The ratio of these two Rayleigh numbers is referred to as the buoyancy ratio

$$Nr = \frac{Ra_C}{Ra_T}.$$

From figure 3(a) it is observed that increasing *Nr*, the isothermal lines at the middle part of the thin layer become more bended whereas initially (Nr = 1) they are sinusoidal wavy pattern due to forming temperature gradient across the layer.

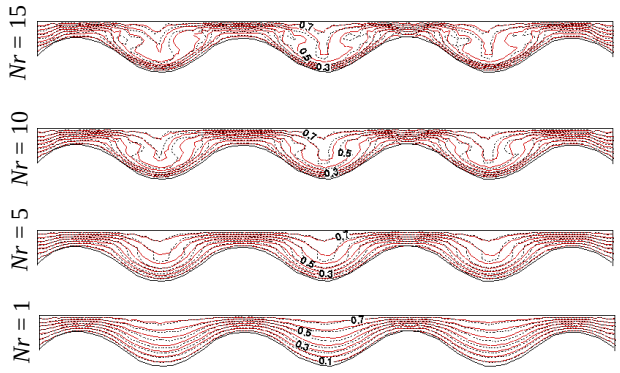

Fig. 3(a): Effect of *Nr* on isothermal lines.

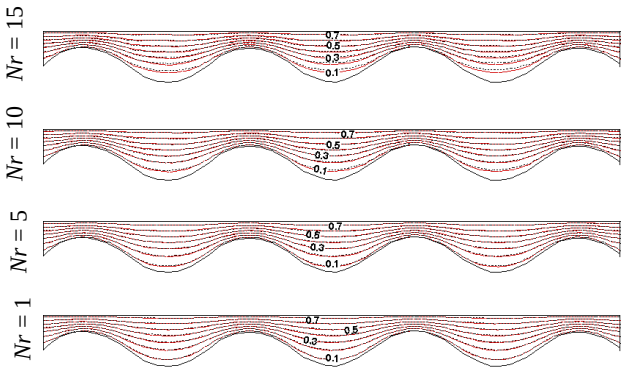

Fig. 3(b): Effect of *Nr* on iso-concentration lines.

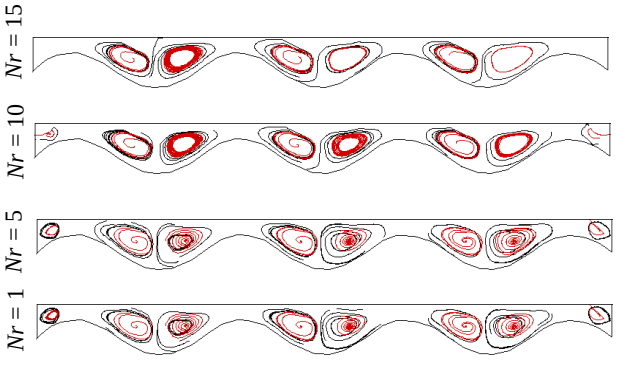

Fig. 3(c): Effect of *Nr* on streamlines.

With the growing values of *Nr*, the temperature distribution becomes distorted resulting in an increase in the overall heat transfer. It is worth noting that as the buoyancy ratio increases, the thickness of the thermal boundary layer adjacent to the wavy area rises which indicates a steep temperature gradient. Hence, an increase in the overall heat transfer within the domain is observed. More variation is seen for water based nanofluid with Cu nanoparticle than clear water.

On the other hand, Fig. 3(b) shows that there is no significant effect in the iso-concentration profile for escalating *Nr* through the wavy thin layer. Also the labeling in the isothermal lines and iso-concentration lines represents the contour number in an order.

Six primary recirculation cells occupying the entire solar collector are found for the absence of the buoyancy ratio (*Nr*) in the Fig. 3(c). As well as two tiny vortices created near the vertical walls for base fluid. The size of these eddies become larger with the increasing of the buoyancy ratio. There creates some perturbation in the streamlines near the top area inside the collector for larger values of *Nr* (= 10 and 15). In addition little vortices near vertical walls disappear at the highest value of buoyancy ratio.

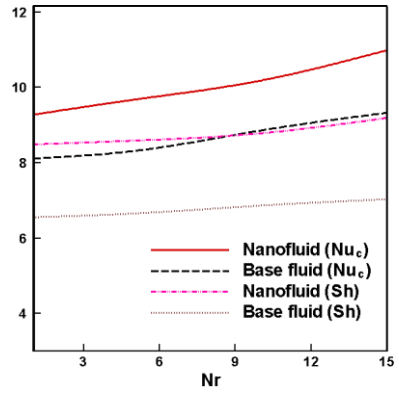

Fig. 4: Rate of heat transfer for the effect of *Nr.*

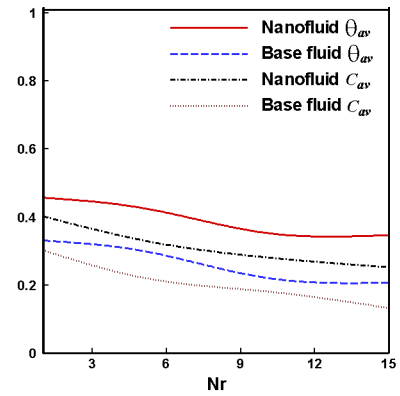

Fig. 5: Mean temperature of fluids for the effect of *Nr.*

The average Nusselt number and mean Sherwood number (*Sh*) profiles along with the various buoyancy ratio (*Nr*) are displayed in Fig. 4. From this figure it is evident that a linear increasing is obtained among heat and mass transfer rates according to the *Nr*. It is also seen that *Nu* and *Sh* enhance gradually more for nanofluid than clear water. Rates of convective heat transfer and mass transfer for nanofluid and base fluid enhance by 15%, 7% and 13%, 6% respectively with the variation of *Nr* from 1 to 15. Also heat transfer rate is higher for nanofluid than clear water. This happens because nanofluid with Cu nanoparticles has more thermal conductivity than base fluid (ϕ = 0%).

Fig. 5 shows the average temperature (θ_{av}) and concentration (C_{av}) for both types of fluids along with the buoyancy (*Nr*). With escalating *Nr* they reduce for base fluid as well as nanofluid. This is due to the fact that temperature and concentration of both type of fluids devalues for the higher values of this governing parameter.

The magnitude of average sub domain velocity field V_{av} inside the thin layer for the influence of buoyancy ratio is exposed in Fig. 6. It is found that a small variation in velocity is due to changing acting parameter. V_{av} grows up gradually with the mounting *Nr*. Base fluid has greater variation than nanofluid as nanofluid with solid concentration cannot move freely.

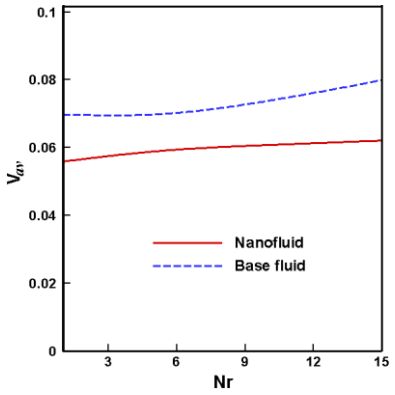

Fig. 6: Average velocity of fluids for the effect of *Nr.*

6. CONCLUSIONS

The following conclusions may be drawn from this article:

- The structure of the fluid streamlines, isotherms and iso-concentrations within the thin layer is found to significantly depend upon the buoyancy ratio.
- The Cu nanoparticles with the highest *Nr* are established to be most effective in enhancing performance of heat-mass transfer rate than base fluid.
- Average temperature and concentration lessen for rising *Nr*.
- Mean velocity increases for base fluid than nanofluid with *Nr* = 15.

REFERENCES

[1] S. Parvin, R. Nasrin, M. A. Alim, and N. F. Hossain, “Double diffusive natural convection in a partially heated enclosure using nanofluid”, Heat Trans.-Asian Res., Vol. 41, No. 6, pp. 484–497, 2012.

[2] S. Parvin, R. Nasrin and M. A. Alim, Heat transfer and entropy generation through nanofluid filled Direct Absorption Solar Collector, Int. J. of Heat and Mass Transf., Vol. 71, pp. 386–395, 2014,

[3] R Nasrin, M. A. Alim and A. J. Chamkha, "Effect of viscosity variation on natural convection flow of water-alumina nanofluid in an annulus with internal heat generation", Heat Transfer-Asian Res., Vol. 41, No. 6, pp. 536–552, 2012.

[4] R. Nasrin and M. A. Alim, "Effect of nanoparticle volume fraction on buoyant flow in a solar collector with undulating absorber", Int. J. of Energy & Tech., Vol. 4, No. 19, pp. 1–9, 2012.

[5] R. Nasrin and M. A. Alim, "Dufour-Soret effects on natural convection inside a solar collector utilizing water-CuO nanofluid", Int. J. of Energy &Tech., Vol. 4, No.23, pp. 1–10, 2012.

[6] R. Nasrin and M. A. Alim, "Aspect ratio effect on convective flow in a solar collector with sinusoidal wavy absorber using nanofluid", Engg. e Transaction, Vol. 7, No. 2, pp. 77–85, 2012.

[7] R. Nasrin, M. A. Alim and A. J. Chamkha, "Effects of physical parameters on natural convection in a solar collector filled with nanofluid", Heat Trans.-Asian Res., Vol. 42, No. 1, pp. 73–88, 2013.

[8] R. Nasrin and M. A. Alim, "Modeling of double diffusive buoyant flow in a solar collector with water-CuO nanofluid", Heat Transfer-Asian Res., Vol. 42, No. 3, pp. 212–229, 2013.

[9] R. Nasrin and M. A. Alim, "Non-darcy assisted flow along a channel with an open cavity filled with water-TiO_2 nanofluid", Heat Transfer-Asian Res., Vol. 42, No. 4, pp. 300–318, 2013.

[10] R. Nasrin and M. A. Alim, "Heat transfer by nanofluid with different nanoparticles in a solar collector", Heat Trans.-Asian Res., Vol. 43, No. 1, pp.61–79, 2014.

[11] R. Nasrin and MA. Alim, "Semi-empirical relation for forced convective analysis through a solar collector", Solar Energy, Vol. 105, pp. 455–467, 2014.

[12] R. Nasrin, S. Parvin and M.A. Alim, "Heat transfer and collector efficiency through direct absorption solar collector with radiative heat flux effect", Num. Heat Transf., Part A- Applications (Accepted).

[13] B. C. Pak and Y. Cho, "Hydrodynamic and heat transfer study of dispersed fluids with submicron metallic oxide particle", Exp. Heat Trans., Vol. 11, pp. 151–170, 1998.

[14] J. C. Maxwell-Garnett, "Colours in metal glasses and in metallic films", Philos. Trans. Roy. Soc. A, Vol. 203, pp. 385–420, 1904.

[15] H. Saleh, R. Roslan, I. Hashim, "Natural convection heat transfer in a nanofluid-filled trapezoidal enclosure", Int. J. of Heat and Mass Trans., Vol. 54, pp. 194–201, 2011.

[16] C. Taylor and P. Hood, "A numerical solution of the Navier-Stokes equations using finite element technique", Computer and Fluids, Vol. 1, pp. 73–89, 1973.

[17] P. Dechaumphai, Finite Element Method in Engineering, 2nd ed., Chulalongkorn University Press, Bangkok, 1999.

[18] E. B. Ogut, "Natural convection of water-based nanofluids in an inclined enclosure with a heat source", Int. J. of Thermal Sciences, Vol. 48, no. 11, pp. 2063–2073, 2009.

[19] N. Nithyadevi and R. J. Yang, "Double diffusive natural convection in a partially heated enclosure with Soret and Dufour effects", Int. J. Heat and Fluid Flow, Vol. 30, pp. 902–910, 2009.